

Comparing performance simulations for Aeolus and Aeolus-2

Uwe Marksteiner¹, Stefanie Knobloch¹, Benjamin Witschas¹, Oliver Reitebuch¹, Markus Meringer², Dorit Huber³, Katja Reissig⁴

¹Institute of Atmospheric Physics, German Aerospace Center DLR, Oberpfaffenhofen 82234, Germany

²Remote Sensing Technology Institute, German Aerospace Center DLR, Oberpfaffenhofen 82234, Germany / ³DoRIT on Research Information Technology, Fürstfeldbruck 82256, Germany / ⁴IB Reissig, Finning 86923, Germany

On **August 22nd, 2018**, the European Space Agency (ESA) launched its Earth Explorer satellite **Aeolus**, which carried the **first wind lidar into space**. It emitted laser pulses at 355 nm and analysed the light, that was Doppler shifted and backscattered by the atmosphere. During its almost **five years of operation** Aeolus provided the first measurements of line-of-sight **wind profiles** between 0 – 30 km on a global scale and in near real time, which showed a significantly and **positive impact on numerical weather prediction**. On July 28th, 2023, ESA successfully performed an **assisted re-entry** of Aeolus, another **world's first**.

Based on the success of Aeolus, the follow-on mission **Aeolus-2** (EPS-Aeolus for EUMETSAT) is planned in cooperation between EUMETSAT and ESA. We reconfigured the existing **Aeolus End-to-End Simulator (E2S)** to evaluate the **radiometric performance** of the Aeolus **Rayleigh** channel by comparing simulated and measured signals, as well as to representatively simulate the planned mission performance of Aeolus-2. Investigations of a **Dual-channel Michelson interferometer (DMI)** were conducted to assess the influence of **Mie contamination** on the Rayleigh channel and the accuracy of its correction.

The Aeolus mission

The objective of the Aeolus mission was to improve numerical weather prediction (NWP) and advance our understanding of atmospheric dynamics and climate processes by considering the obtained wind measurements. The associated Doppler frequency shifts of cloud/aerosol and molecular backscatter were derived from two complementary receiver channels (Mie and Rayleigh), each employing an accumulation charge-coupled device (ACCD).

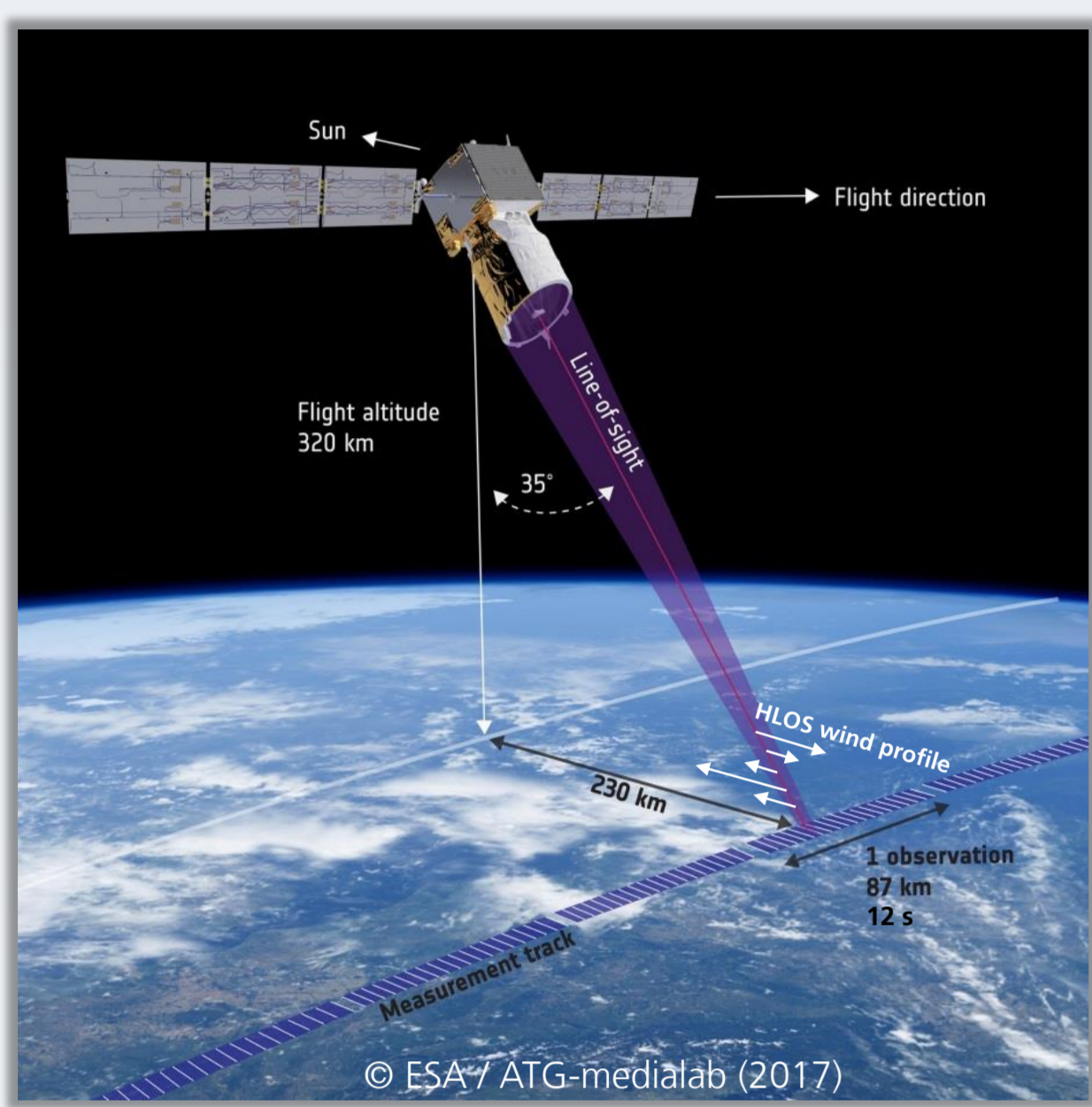


Fig. 1: Viewing geometry and sampling strategy of the Aeolus satellite for horizontal line-of-sight (LOS) wind speed (adapted).

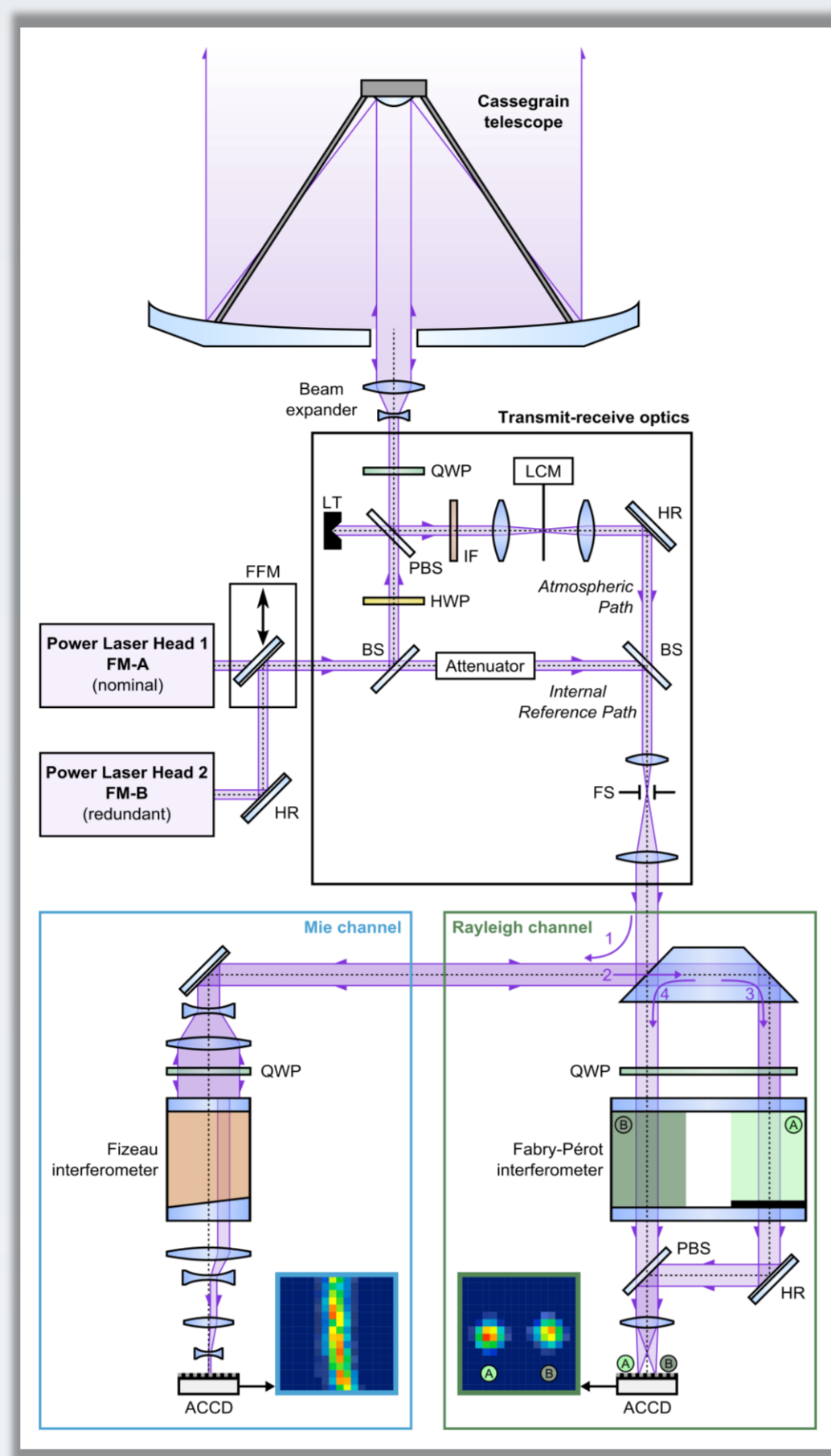


Fig. 2: Schematic of the lidar on board Aeolus, with two redundant lasers, a telescope, transmit receive optics and a dual-channel receiver [1].

The Aeolus End-to-End Simulator (E2S)

By considering the detailed technical characteristics of the instrument as well as **user defined** atmospheric conditions, the E2S produces Rayleigh and Mie signal data. Together with albedo and digital elevation model information as well as housekeeping and ephemeris data the **E2S** then creates **output** files with the same **format** as provided by the **Aeolus satellite**. The E2S was used extensively in combination with the Aeolus L1B, L2A and L2B processors **before launch** for performance simulations, algorithm sensitivity studies and functional testing over 15 years. **After launch**, the E2S was for example used for estimation of initial signal loss.

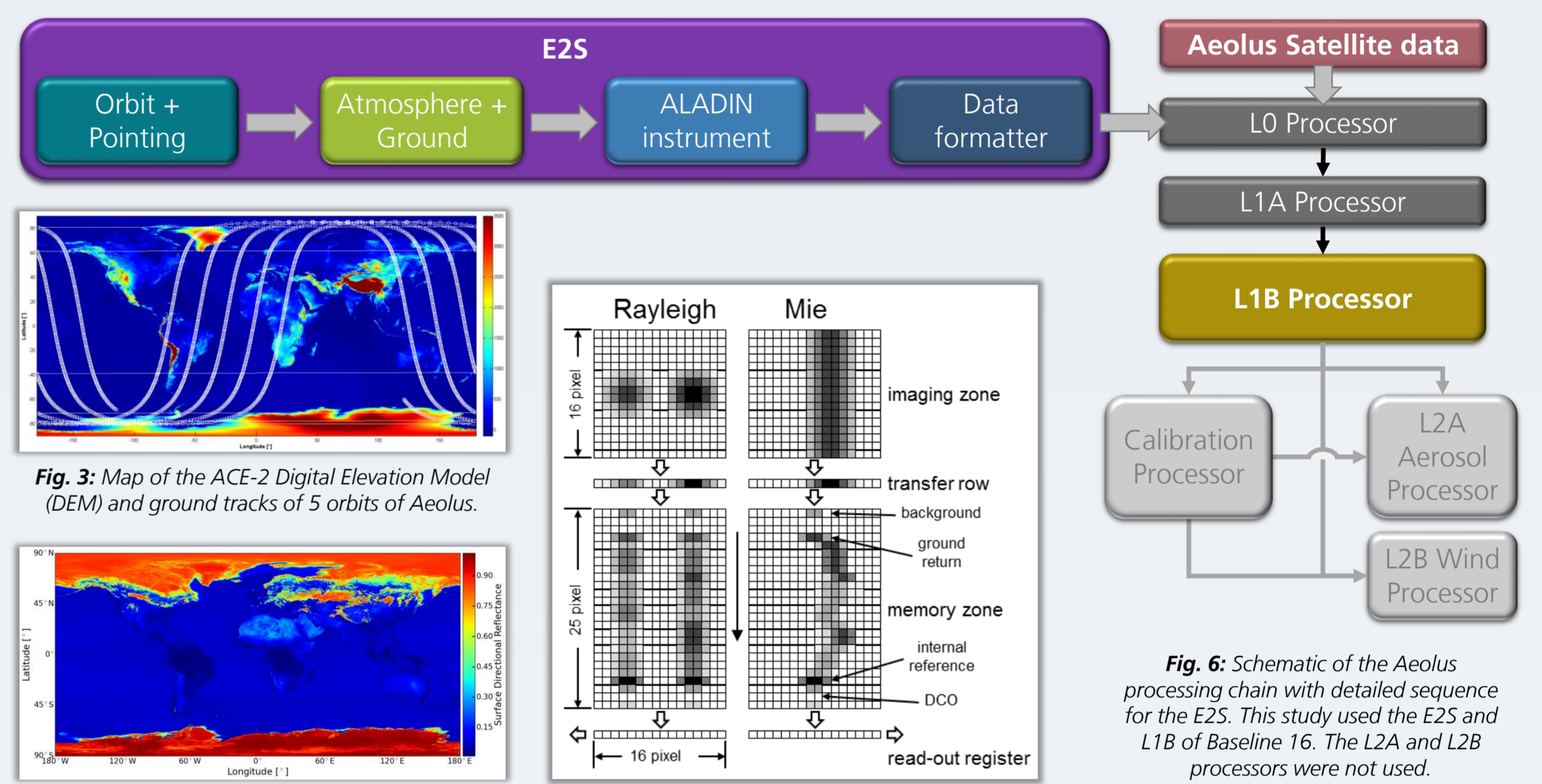


Fig. 3: Map of the ACE-2 Digital Elevation Model (DEM) and ground tracks of 5 orbits of Aeolus.

Fig. 4: Adapted map of UV surface albedo based on ESA's ADAM database v.3.0.

Fig. 6: Schematic of the Aeolus processing chain with detailed sequence for the E2S. This study used the E2S and L1B of Baseline 16. The L2A and L2B processors were not used.

Updates of the E2S configuration in view of Aeolus-2

Table 1: Selection of relevant parameters as used for performance simulation of Aeolus and Aeolus-2.

| Parameter | Aeolus | Aeolus-2 |
|----------------------------|-----------------------------|--------------------|
| Orbit altitude | ≈ 320 km | ≈ 400 km |
| Vertical measurement range | 0 – 25 km | 0 – 40 km |
| Vertical resolution | 250 m – 2000 m | 125 m – 2000 m |
| Number of range-gates | 24 (+1 background) | 66 (+1 background) |
| Laser energy | varying: ≈ 35 mJ – 100 mJ | 150 mJ |
| DEM | ACE-2 and Copernicus GLO-90 | Copernicus GLO-90 |

- Further **differences** between the simulations of Aeolus and Aeolus-2 as well as the real Aeolus measurements were considered in terms of orbit related parameters and individual calibration files applied during the wind retrieval with the L1B processor.
- For the simulations the **transmission** values for the transmit and the receive path were **adapted** according to the evolution of the observed Aeolus signal losses throughout the mission lifetime. The aim was to correlate the Rayleigh signal measured in-orbit to those simulated with the E2S.
- Therefore, **8 different measurement sections** were selected. These are distributed such, that they reflect all major periods of the mission, notably the FMA-1/2 and FMB laser periods and periods of low, medium and high laser energy. To cover the atmospheric variability, the mostly cloud free (→ Rayleigh) sections exhibit very weak and very strong horizontal and vertical wind gradients and a large range of wind speeds.



Fig. 7: 8 scenarios as measured by Aeolus between 2018-09-22 (1) and 2023-04-30 (8) and selected for simulation and comparison.

Comparison of E2S simulations to Aeolus and Aeolus-2

As a first step, towards an end-to-end simulator for Aeolus-2 it is needed to achieve **consistency** between **simulation** and **measurement** for **Aeolus** in terms of the atmospheric signal levels and the wind random error.

Almost **no altitude-dependent error** remains in the ratio of the Rayleigh signal from E2S simulation and Aeolus measurements if the actual atmospheric temperature profiles are used as input to the simulations. On observation resolution the **E2S** produces **less variability** in Rayleigh signal than what is observed from **Aeolus measurements**.

By scaling to the requirements on horizontal and vertical resolution in the different atmospheric layers, the wind random error of **Aeolus-2** like simulations can be compared to the respective wind precision requirements:

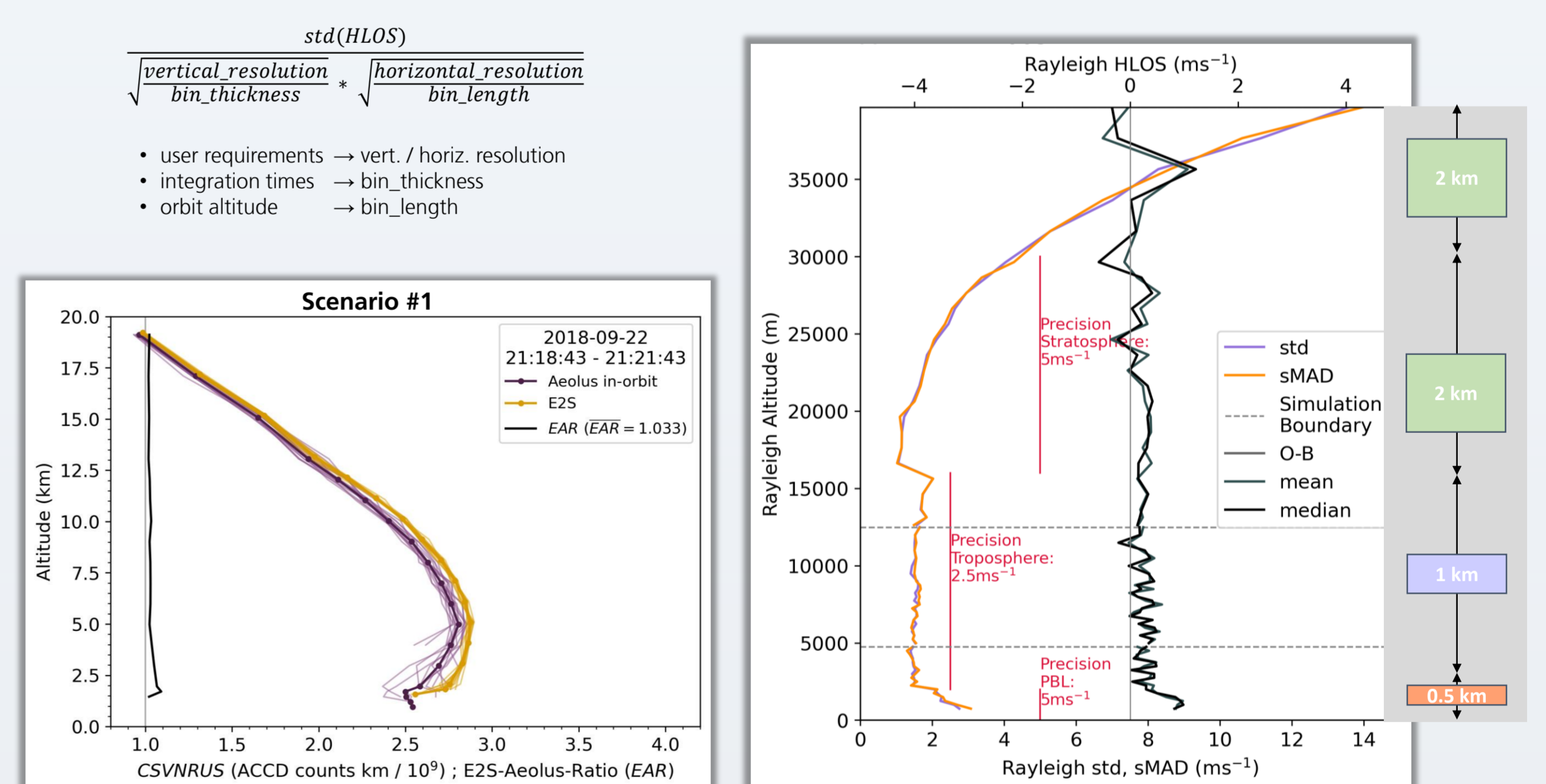


Fig. 8: Vertical profiles of clear sky valid normalized Rayleigh useful signal from Aeolus measurements (violet) and E2S (orange) as well as the E2S-Aeolus ratio profile (black). Thick lines show the mean values. A realistic atmosphere in terms of pressure, temperature and wind derived from the ECMWF model was considered. A tuning factor was applied according to the signal decay observed during the mission.

Fig. 9: L1B Rayleigh HLOS wind bias (black) from comparison against the E2S input wind profile and random error for Aeolus-2 simulations (with simplified atmosphere). The user requirements on threshold level (red) are given for the planetary boundary layer (PBL), the troposphere and the stratosphere. The random errors are scaled to the corresponding range-gate resolutions (right) of the user requirements.

Dual-channel Michelson vs. Fabry-Pérot Interferometer

- A representative model of a Dual-channel Michelson Interferometer (**DMI**) was developed for Aeolus-2 as an alternative to the established Fabry-Pérot Interferometer (**FPI**).
- The sensitivity to **narrowband** signals (particulate return) turned out to be very **similar** for FPI & DMI.
- The sensitivity to **broadband** signals (molecular return) turned out to be significantly **lower** for the DMI than for the FPI.
- Mie contamination** on the Rayleigh signal is a **significant error contributor** for 1.3 < scattering ratio < 2.0 (depending on atmospheric temperature).
- In regions where Mie SNR is too low to derive accurate Mie winds (intermediate SR regime) a **“correction” of Rayleigh winds** is needed [2] (→ critical for DMI).
- The better the accuracy of the knowledge on the **scattering ratio (SR)** the lower the **Mie** sensitivity error and the lower the **wind speed dependent error** after the correction applied to the Rayleigh winds.
- In case of insufficient SR-knowledge contaminated Rayleigh winds must be **flagged** invalid.

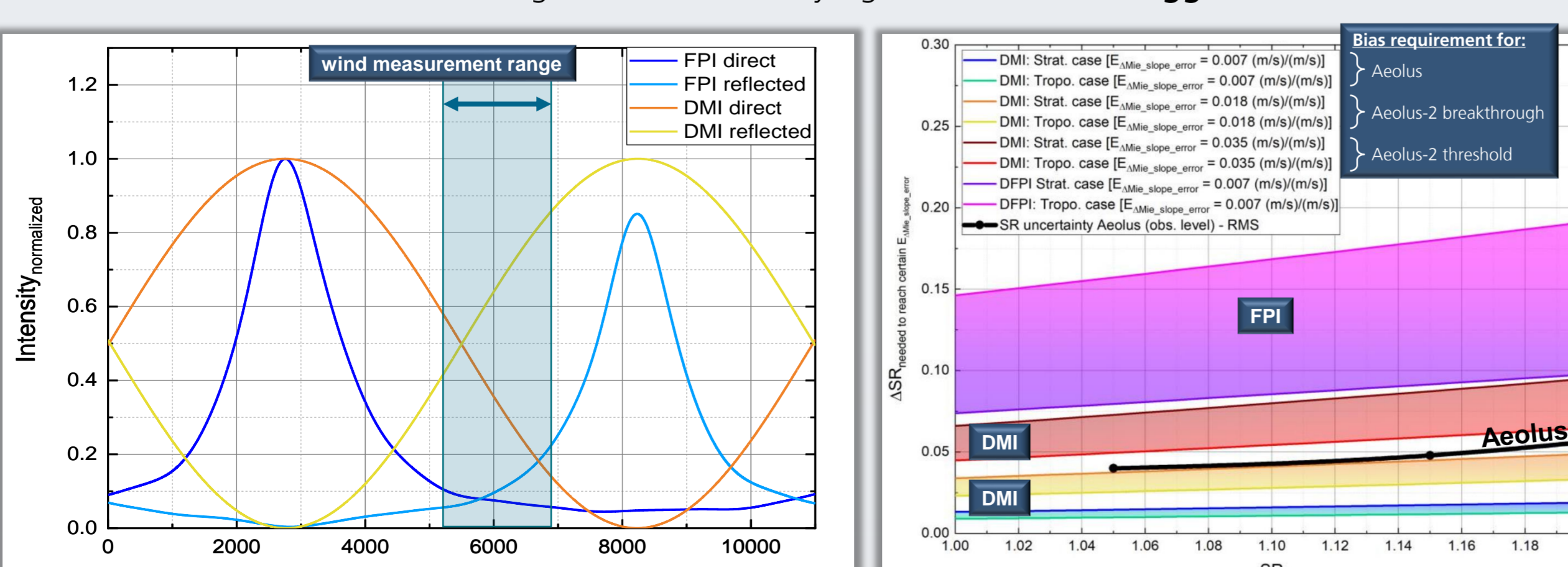


Fig. 10: Transmission curves over the full free spectral range of the FPI and DMI for the internal reference path derived under basic assumptions (e.g. without considering reflection at the Fizeau).

Fig. 11: Needed knowledge on SR precision ΔSR to reach certain Mie slope errors when using the DMI or the FPI. Colored regions show the dependence on atmospheric temperature & pressure (troposphere → stratosphere). ΔSR as known from Aeolus is given in black.

Conclusions

- Considering realistic atmosphere and the knowledge about the performance of the Aeolus instrument during operation, the **E2S** is capable of reproducing the **Rayleigh useful signal** profiles of real **Aeolus** measurements with deviations of less than 5%.
- The **E2S** was **updated** such that it can reflect the basic parameters of **Aeolus-2** according to the current state of knowledge, including amongst others the higher orbit altitude, the larger number of range-gates, the improved range-gate resolution and the stronger laser.
- With the current **configuration** of the **E2S** regarding **Aeolus-2** the corresponding user threshold **requirements can be met**. However, this result is still based on an orbit altitude of 400 km (will be 450 km), simplified atmosphere, a disregard of the impact of the solar background.
- A performance comparison of **Fabry-Pérot** and **Dual-Michelson Interferometers** revealed significant disadvantages of the latter in terms of scattering ratio determination and, hence, cross-talk correction and Rayleigh wind precision. These results supported the decision to keep the FPI as Rayleigh spectrometer.
- Future improvements** of the E2S should focus on the simulation of, amongst others, the Co-Alignment Sensor, the Beam-Steering Mechanism, more realistic bias variations along the orbit, the Rayleigh channel spots, the Rayleigh solar background, the ground detection algorithm.

Funding for this study was provided by **EUMETSAT**.



[1] Lux et. al., "ALADIN laser frequency stability and its impact on the Aeolus wind error", AMT, Vol. 14-9, 6305-6333 (2021)
[2] Dabas et al., "Correcting winds measured with a Rayleigh Doppler lidar from pressure and temperature effects", Tellus, 60A, 206-215 (2008)